

Robust Quantum Control for Bragg Pulse Design in Atom Interferometry

Luke S. Baker¹, Andre Luiz P. de Lima^{1,2}, Andrew Harter¹, Ceren Uzun¹,

Jr-Shin Li², Anatoly Zlotnik¹, Michael J. Martin¹, Malcolm G. Boshier¹

¹Los Alamos National Laboratory, ²Washington University in St. Louis

(Dated: February 11, 2025)

We formulate a robust optimal control algorithm to synthesize minimum energy pulses that can transfer a cold atom system into various momentum states. The algorithm uses adaptive linearization of the evolution operator and sequential quadratic programming to iterate the control towards a minimum energy signal that achieves optimal target state fidelity. Robustness to parameter variation is achieved using Legendre polynomial approximation over the domain of variation. The method is applied to optimize the Bragg beamsplitting operation in ultra-cold atom interferometry. Even in the presence of 10-40% variability in the initial momentum dispersion of the atomic cloud and the intensity of the optical pulse, the algorithm reliably converges to a control protocol that robustly achieves unprecedented momentum levels with high fidelity for a single-frequency multi-photon Bragg diffraction scheme (e.g. $|\pm 40\hbar k\rangle$). Advantages of the proposed method are demonstrated by comparison to stochastic optimization using sampled parameter values.

Algorithms for optimal quantum control have been advanced and generalized during the past decades, and enable the current emergence of high-precision quantum circuits and sensing architectures [1]. Established algorithms such as Gradient Ascent Pulse Engineering (GRAPE) [2] iteratively adjust a control pulse towards one that maximizes the likelihood of realizing a target state with optimal fidelity. Ensuring that the designed signal is resilient to noise and platform disturbance within a design region is also important for practical quantum-enhanced sensing routines [3]. While stochastic sampling has been shown to improve resilience [4], a robust control approach that provides guarantees over a wide range of disturbances is highly desirable conceptually and computationally. In this letter we augment optimal quantum control with robustness guarantees using spectral approximation over the domain of parameter variation [5], and introduce a powerful algorithm with improved performance and resilience. The algorithm is derived for general closed quantum systems and is showcased with numerical simulations involving atom interferometry. Potential extensions to general systems driven by energy exchange and decoherence are possible [6].

Consider a closed quantum system over a finite-dimensional Hilbert space in which the wave vector evolves according to the Schrödinger equation

$$i\hbar \frac{d|\Psi(t)\rangle}{dt} = \left(\gamma_0 \mathcal{H}_0 + \sum_{m=1}^M \gamma_m u_m(t) \mathcal{H}_m \right) |\Psi(t)\rangle. \quad (1)$$

The evolution of the state is influenced by control variables $u_m(t)$ that represent the amplitudes of electromagnetic fields applied on the system. Each variable parameter γ_m is capable of assuming any value in a specified closed interval denoted by $[\gamma_m^{\min}, \gamma_m^{\max}]$. These parameters are used to compensate for external disturbances, including miscalibration and platform noise, that may appear as parameter variability within the static component of the Hamiltonian and the amplitudes of the ap-

plied fields. For ease of exposition, we follow previous approaches and assume that the Hamiltonian depends linearly on these parameters [2]. The above formulation warrants the design of control signals that are robust or insensitive to coherent errors and therefore can be used to model a broad range of desirable applications in atom interferometry [7–10], quantum computing [11], and nuclear magnetic resonance spectroscopy [12].

The parameterized Hamiltonian governs the evolution of a finite-dimensional wave vector dependent on a continuum of parameter values. A common approach for reduction to a finite-dimensional representation is based on direct [2] or random [4, 13] sampling over the parameter intervals. In this letter, we propose an alternative method of moments in which the wave vector is expanded over products of Legendre polynomials. By truncating the expansion to polynomials of sufficiently high degrees, we obtain an approximate representation of the form

$$|\Psi\rangle = \sum_{n_0, \dots, n_M=0}^{N_0, \dots, N_M} |\psi_{n_0, \dots, n_M}(t)\rangle \ell_{n_0}(\gamma_0) \cdots \ell_{n_M}(\gamma_M), \quad (2)$$

where $\ell_n(\gamma_m)$ represents the normalized Legendre polynomial of degree n with the domain shifted to the interval $[\gamma_m^{\min}, \gamma_m^{\max}]$. Because of exponential decay properties of Legendre expansions [5], the method of moments may promote a more rapid convergence rate than sampling and can yield more accurate representations with only a small number of polynomials. This advantage will be demonstrated in the examples below. The dynamical evolution of a particular ordering of the coefficient vectors is governed by [14]

$$i\hbar \frac{d|\psi(t)\rangle}{dt} = \left(H_0 + \sum_{m=1}^M u_m(t) H_m \right) |\psi(t)\rangle, \quad (3)$$

where H_m is a multilevel Kronecker product extension of \mathcal{H}_m . Our subsequent analysis is developed using the robust representation in Eq. (3).

We formulate an optimal control algorithm to actuate a robust evolution from a prepared initial state $|\psi_0\rangle$ to a specified target state $|\psi_T\rangle$ over a desired time interval $[0, T]$. We assume for simplicity that the chosen time of application is discretized into K equal steps of duration $\Delta t = T/K$. In the event that the control signals are constant during each step $[t_k, t_{k+1})$, the wave vector in Eq. (3) evolves according to $|\psi_{k+1}\rangle = U_k|\psi_k\rangle$, where the unitary operators are defined by

$$U_k = \exp\left(-\frac{i\Delta t}{\hbar}\left(H_0 + \sum_{m=1}^M u_m(t_k)H_m\right)\right). \quad (4)$$

The subscript k indicates the evaluation at time t_k of the quantity to which it associates. Successively applying the single time-step transition results in a terminal state probed by the selected controls of the form

$$|\psi_K\rangle = U_{K-1}U_{K-2}\cdots U_1U_0|\psi_0\rangle. \quad (5)$$

The control algorithm derived in the following is based on adaptive linearization of this nonlinear evolution equation together with iterative quadratic programming.

For each k , define $\mathbf{u}_k = (u_0(t_k), u_1(t_k), \dots, u_M(t_k))'$ and use the time sampled vector to construct the control vector $u = (\mathbf{u}'_0, \mathbf{u}'_1, \dots, \mathbf{u}'_{K-1})'$, where the prime $'$ denotes the transpose operation. Likewise, define the matrices

$$J_k = \left(\frac{\partial|\psi_K\rangle}{\partial u_0(t_k)}, \frac{\partial|\psi_K\rangle}{\partial u_1(t_k)}, \dots, \frac{\partial|\psi_K\rangle}{\partial u_M(t_k)}\right), \quad (6)$$

and construct the Jacobian $J = (J_0, J_1, \dots, J_{K-1})$. Given a signal u and the corresponding terminal state $|\psi_K\rangle$ computed using Eq. (5), the control algorithm seeks to update the signal $u \rightarrow u + \delta u$ in such a way that the updated terminal state $|\psi_K\rangle \rightarrow |\psi_K\rangle + |\delta\psi_K\rangle$ improves the objective to optimize. Although other objectives may be formulated, we consider minimization of the terminal error $\|\psi_K - \psi_T\|^2 = \langle\psi_K - \psi_T|\psi_K - \psi_T\rangle$. To first order, the updates are related through the linear representation

$$|\delta\psi_K\rangle = J\delta u. \quad (7)$$

Because this iterative updating is standard for gradient-based methods, the simulation in Eq. (5) and the Jacobian J may be computed by existing methods [15, 16].

As an alternative to gradient updates, δu is defined to be the solution of the quadratic program given by

$$\begin{aligned} \text{minimize: } & \|J\delta u + \psi_K - \psi_T\|^2 + \lambda\|\delta u\|^2 \\ \text{subject to: } & \text{signal restrictions.} \end{aligned} \quad (8)$$

An advantage of this formulation is that it directly enables the user to define signal restrictions in the form of inequality constraints. Signal restrictions refer to specified lower and upper bounds on any finite number of linear combinations of the components of the control vector. These restrictions are considered to be a practical feature

of the proposed algorithm because they can ensure an engineered outcome in which the intensity, spectrum, and potentially total energy of the prepared signal may be directly restricted to comply with equipment operating limits. A positive regulation parameter λ is introduced into the objective to restrict the size of the update between iterations. By choosing λ sufficiently large, the local dynamics and hence the accuracy of linearization can be regulated to arbitrary precision. The algorithm begins by choosing a random control signal u that satisfies the imposed restrictions and a sufficiently large value for λ which is subsequently decreased as a function of iteration count if the difference between two successive objective values falls below a specified threshold. The algorithm terminates whenever the error reaches a specified tolerance.

A signal of minimum energy is usually synthesized by introducing penalty terms to the objective function in Eq. (8). Because this approach could lead to competition between signal energy and terminal state fidelity, we resolve this trade-off by formulating a minimum energy control algorithm that is applied in stages to first maximize terminal state fidelity by way of problem (8) and then minimize control energy while achieving the same fidelity. For the latter, the control signal is gradually adjusted with subsequent iterations of the quadratic program [17]

$$\begin{aligned} \text{minimize: } & \|u + \delta u\|^2 + \mu\|\delta u\|^2, \\ \text{subject to: } & PJ\delta u = 0, \\ & \text{signal restrictions,} \end{aligned} \quad (9)$$

where μ serves the same purpose as λ from the previous algorithm. Using Eq. (7), the equality constraint $PJ\delta u = 0$ ensures that the terminal state fidelity achieved with the robust optimal control algorithm is preserved as the minimum energy algorithm progresses through its iterations. In this way, fidelity is not affected by minimizing signal energy. The matrix P represents a projection onto the space orthogonal to the target state to provide the minimum energy algorithm with flexibility to alter the phase of the target state for fixed magnitude in probability. Although the optimal robust and minimum energy algorithms are presented individually, we note that they may be integrated into one algorithm that solves both quadratic programs (8)-(9) in succession with each iteration. Another approach may cycle between the two algorithms and apply an adaptive number of iterations before switching back to the other. Such algorithmic extensions are beyond the scope of this letter.

The robust and minimum energy control algorithms will be applied to design beamsplitters in ultra-cold atom interferometry. Beamsplitters often rely on multi-photon Bragg scattering, where counter-propagating laser beams form a standing-wave that coherently transfers momentum to atoms, splitting their wave packets into distinct momentum states. This process forms the foundation of

atom interferometry by creating the necessary path separation for interference measurements. Recent efforts utilize rectangular, triangular, and Gaussian pulse signals [7, 18–21], in which the intensity and duration of pulses are typically treated as optimization variables. Although these designs may be appealing, predefined signal shapes can severely limit the space over which the optimizer seeks a solution, potentially resulting in sub-optimality and low fidelity. To improve fidelity, robust optimal control has recently been applied to design beamsplitting pulses [8, 14, 22], with which experimental advantage over some contemporary methods has been demonstrated [8]. However, a reliable method for designing robust pulses capable of realizing high momentum beamsplitters with high fidelity is still an open challenge.

The evolution of a sample of ultra-cold atoms in a one-dimensional standing-wave potential is assumed to be governed by the Schrödinger equation [18, 21]

$$i \frac{\partial \Psi}{\partial t} = -\frac{\hbar}{2m} \frac{\partial^2 \Psi}{\partial x^2} + u(t) \cos(2k_0 x) \Psi, \quad (10)$$

where $u(t)$ is the amplitude of the light shift potential and k_0 is the vacuum wave number of the photons. Although additional control variables may enable even higher fidelity, we assume control of only optical intensity and use this stage to highlight the capabilities of the controller to such limited control. Eliminating the need for additional control variables to achieve high-order Bragg splitting reduces experimental complexity, which distinguishes our approach from that described in Refs. [8, 9], where parameters such as the relative detuning and phase of the counter-propagating beams are controlled. By expanding $\Psi(t, x) = \sum_n \int d\mathbf{k} C_{2n}(t, \mathbf{k}) e^{i(2nk_0 + k)x}$ in the momentum basis and substituting the superposition into Eq. (10), the evolution of the coefficients may be expressed as [18]

$$i \dot{C}_{2n} = \omega_r \left(2n + \frac{k}{k_0} \right)^2 C_{2n} + \gamma \frac{u(t)}{2} (C_{2n-2} + C_{2n+2}), \quad (11)$$

where $\omega_r = \hbar k_0^2 / 2m$ is the photon recoil frequency. The parameters k/k_0 and γ are considered variable over respective ranges to compensate for variation of momentum across the atomic population and optical intensity, respectively. The set of scalar equations indexed by the momentum level n is truncated with integral steps from $n = -N$ to $n = N$. It will be clear from context whether k and n denote conventional quantities in atom interferometry or the above time step and Legendre polynomial indices. By specifying a target momentum level $n_0 \ll N$, the controller seeks a robust pulse that probes the atomic cloud from the initially prepared zero momentum state $|0\hbar k\rangle$ to the excited state $|\pm 2n_0 \hbar k\rangle$, where $|2n\hbar k\rangle = C_{2n}$.

Several studies are performed to demonstrate various properties of the control algorithm. First, convergence is analyzed for the deterministic case in which nominal parameter values $k/k_0 = 0$ and $\gamma = 1$ are fixed. Sec-

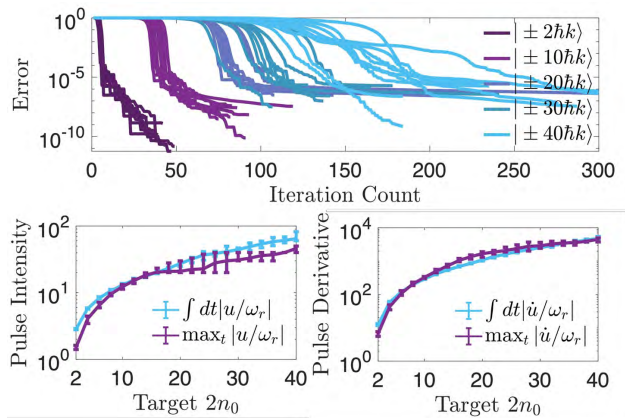


FIG. 1: Top: Convergence of the iterative algorithm for selected target momenta $|\pm 2n_0 \hbar k\rangle$. Bottom: Maximum and mean values for control amplitude and derivative.

ond, three beamsplitting examples that compensate for 10% variation in $k/k_0 \in [-0.1, 0.1]$ and $\gamma \in [0.9, 1.1]$ are presented to visualize additional properties of the controller. Third, comparison to the direct sampling approach to robustness is documented for three additional beamsplitting examples that compensate for 40% variation in $k/k_0 \in [-0.4, 0.4]$ and $\gamma \in [0.6, 1.4]$. All results are obtained by optimization in dimensionless time $\omega_r t$ over the interval $[0, 2\pi]$ using 630 time steps. Computations are performed in Matlab on a MacBook Pro.

Figure 1 displays the results of pulse designs that achieve target momentum states ranging from $|2\hbar k\rangle$ to $|40\hbar k\rangle$, where the performance of ten realizations corresponding to ten random initializations of the control signal are shown. Because high momentum beamsplitting targets challenge convergence of both optimal control and conventional methods, we devise a novel application of the proposed algorithm and use it to demonstrate that realization of high momentum beamsplitters with high fidelity can be achieved reliably. The algorithm is applied starting with each random initialization and terminates at a local minimum for the minimum energy control pulse that achieves beamsplitting in the first momentum state $|\pm 2\hbar k\rangle$. The method then uses the resulting solution to initialize the algorithm for beamsplitting to the $|\pm 4\hbar k\rangle$ momentum state. The process is continued until the desired momentum state $|\pm 2n_0 \hbar k\rangle$ is achieved. Figure 1 illustrates that this approach is reliable for realizing high momentum beamsplitters with high fidelity. The minimum energy design is also evident [18].

Figure 2 shows three examples along the top, middle, and bottom rows, respectively, for beamsplitting into target states $|\pm 2\hbar k\rangle$, $|\pm 10\hbar k\rangle$, and $|\pm 20\hbar k\rangle$. Each row displays the control signal, the probability evolution of momentum states, and the terminal error with respect to the desired state. The probability evolution and terminal error realizations are obtained by simulating Eq. (11) applying the computed signal repeatedly for samples

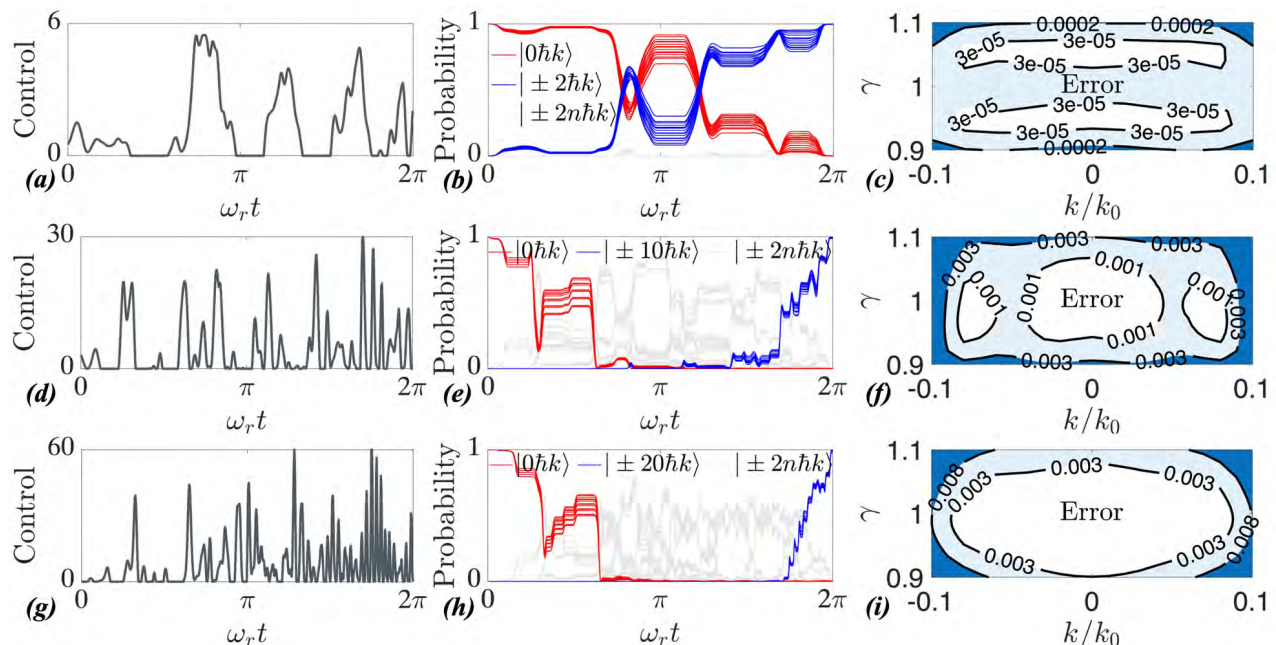


FIG. 2: Beamsplitting from $|0\hbar k\rangle$ to $|\pm 2n_0\hbar k\rangle$, for $n_0 = 1, 5, 10$. Control and probability refer to the quantities u/ω_r and $\| | + 2n\hbar k\rangle \|^2 + \| | - 2n\hbar k\rangle \|^2$. Error refers to the evaluation of $1 - \| | + 2n_0\hbar k\rangle \|^2 - \| | - 2n_0\hbar k\rangle \|^2$ at $t = T$.

of k/k_0 and γ in their respective intervals. The control signal $u(\omega_r t)/\omega_r$ is restricted to positive values less than 30 for $|\pm 10\hbar k\rangle$ and less than 60 for $|\pm 20\hbar k\rangle$. Observe that the maximum amplitudes of signals computed with the robust formulation as presented in Figure 2 are larger than the amplitudes of the deterministic counterparts in Figure 1. Moreover, while still negligible for experiments, the terminal error is greater as a consequence of enforcing compensation for variation over a range of parameter values. Although slightly higher fidelity may be achieved by using higher order polynomial approximation, these three examples use a Legendre expansion truncated up to only first degree polynomials to emphasize the significance of this approach. Uniform fidelity on the parameter space is generally not achievable with robust optimization using sampled systems of equivalent sizes, which in this case correlates to two samples over both parameter intervals.

To illustrate this last claim, we conclude with three examples that begin to exercise the capacity of robust control in which both parameters k/k_0 and γ are now permitted to assume values with 40% variability. Such significant variations are particularly relevant for atom interferometry experiments in which the cloud of ultra-cold atoms does not necessarily realize Bose-Einstein condensation together with considerable susceptibility of signals to platform disturbance. The following examples split the atomic sample into momentum states $|\pm 2\hbar k\rangle$, $|\pm 4\hbar k\rangle$, and $|\pm 6\hbar k\rangle$ with 40% variability in k/k_0 and γ . For each example, the control algorithm is performed with several robust Legendre polynomial expansions truncated respectively to first, second, third, and fourth degree polynomials. The results are documented in Table I.

Moreover, robust pulse designs for these same examples are also synthesized using the alternative approach of uniformly sampling parameter values in the dynamic constraints, and the results are given in Table II. By increasing the degree of Legendre polynomials and the number of samples, the error metrics generally decrease for both methods, but the mean and maximum errors achieved with the proposed Legendre approximation approach decrease at a significantly higher rate than those afforded by direct sampling. The results suggest that Legendre expansion provides an alternative avenue toward robustness that has advantage over direct sampling in terms of error metrics and total computational time.

Acknowledgements—This project was supported by the LDRD program and the Center for Nonlinear Studies at Los Alamos National Laboratory. Research conducted at Los Alamos National Laboratory is done under the auspices of the National Nuclear Security Administration of the U.S. Department of Energy under Contract No. 89233218CNA000001. Report No.: LA-UR-25-20049.

- [1] J. Berberich and D. Fink, Quantum computing through the lens of control: A tutorial introduction, *IEEE Control Systems* **44**, 24 (2024).
- [2] N. Khaneja, T. Reiss, *et al.*, Optimal control of coupled spin dynamics: design of NMR pulse sequences by gradient ascent algorithms, *Journal of Magnetic Resonance* **172**, 296 (2005).
- [3] C. L. Degen, F. Reinhard, and P. Cappellaro, Quantum sensing, *Reviews of modern physics* **89**, 035002 (2017).
- [4] R.-B. Wu, H. Ding, D. Dong, and X. Wang, Learning robust and high-precision quantum controls, *Physical Re-*

TABLE I: Compensation using Legendre expansion with 40% variation in $k/k_0 \in [-0.4, 0.4]$ and $\gamma \in [0.6, 1.4]$.

Poly. Degree/Interval	$ \pm 2\hbar k\rangle$				$ \pm 4\hbar k\rangle$				$ \pm 6\hbar k\rangle$			
	1	2	3	4	1	2	3	4	1	2	3	4
max Error	0.69	0.45	0.17	0.22	0.92	0.69	0.33	0.31	0.96	0.77	0.83	0.58
mean Error	0.24	0.05	0.03	0.02	0.42	0.17	0.09	0.08	0.47	0.31	0.32	0.25
min Error	5e-4	7e-4	1e-3	4e-4	2e-3	1.2e-2	1.0e-2	1.2e-2	3e-3	2.6e-2	2e-2	3.3e-2
max u_k/ω_r	8.7	15.2	18.6	23.3	35.0	34.2	27.3	33.0	41.2	35.6	39.2	33.1
mean u_k/ω_r	2.2	2.5	2.5	2.6	3.2	3.7	3.7	3.6	4.1	4.4	4.6	4.4
max $ \Delta u_k /\omega_r$	1.1	7.5	10.3	15.6	13.5	14.3	13.1	18.8	17.6	17.4	16.7	15.5
mean $ \Delta u_k /\omega_r$	0.20	0.39	0.48	0.58	1.35	1.21	1.08	1.06	1.90	1.67	1.62	1.57
Clock (min)	0.7	4.2	11.5	23.6	4.9	7.4	19.9	37.4	5.6	9.3	22.9	55.7

TABLE II: Compensation using equidistant sampling with 40% variation in k/k_0 and γ .

No. Samples/Interval	$ \pm 2\hbar k\rangle$				$ \pm 4\hbar k\rangle$				$ \pm 6\hbar k\rangle$			
	2	3	4	5	2	3	4	5	2	3	4	5
max Error	0.94	0.75	0.61	0.34	0.99	0.90	0.73	0.87	0.97	0.96	0.96	0.94
mean Error	0.32	0.28	0.14	0.06	0.50	0.36	0.29	0.20	0.64	0.53	0.39	0.28
min Error	1e-9	3.6e-3	6.7e-3	5.8e-3	2e-10	1.5e-2	5.6e-2	2.3e-2	2e-9	1.3e-2	2.5e-2	2.8e-2
max u_k/ω_r	10.9	15.5	18.0	18.8	27.1	22.6	21.9	24.5	37.1	38.1	36.4	35.6
mean u_k/ω_r	1.6	2.2	2.8	2.6	3.3	4.1	4.4	5.0	4.7	4.9	4.8	4.9
max $ \Delta u_k /\omega_r$	1.4	4.0	4.0	4.9	9.9	8.7	8.9	9.6	11.5	14.1	15.4	17.1
mean $ \Delta u_k /\omega_r$	0.19	0.29	0.37	0.43	0.94	0.93	0.91	1.00	1.09	1.43	1.33	1.40
Clock (min)	0.6	3.0	6.5	14.5	3.4	5.9	9.3	23.7	1.1	5.1	13.1	35.9

view A **99**, 042327 (2019).

- [5] H. Wang and S. Xiang, On the convergence rates of Legendre approximation, *Mathematics of Computation* **81**, 861 (2012).
- [6] T. Schulte-Herbrüggen *et al.*, Optimal control for generating quantum gates in open dissipative systems, *Journal of Physics B: Atomic, Molecular and Optical Physics* **44**, 154013 (2011).
- [7] Y.-J. Wang, D. Z. Anderson, V. M. Bright, E. A. Cornell, Q. Diot, T. Kishimoto, M. Prentiss, R. A. Saravanan, S. R. Segal, and S. Wu, Atom Michelson interferometer on a chip using a Bose-Einstein condensate, *Physical Review Letters* **94**, 090405 (2005).
- [8] J. C. Saywell, M. S. Carey, *et al.*, Enhancing the sensitivity of atom-interferometric inertial sensors using robust control, *Nature Communications* **14**, 7626 (2023).
- [9] G. Louie, Z. Chen, T. Deshpande, and T. Kovachy, Robust atom optics for Bragg atom interferometry, *New Journal of Physics* **25**, 083017 (2023).
- [10] V. E. Colussi, J. Copenhaver, M. Seifert, M. Perlin, and M. Holland, Machine learning designed optical lattice atom interferometer, in *Quantum Sensing, Imaging, and Precision Metrology II*, Vol. 12912 (2024) pp. 143–147.
- [11] D. P. DiVincenzo, Quantum computation, *Science* **270**, 255 (1995).
- [12] K. F. Morris and C. S. Johnson Jr., Diffusion-ordered two-dimensional nuclear magnetic resonance spectroscopy, *J. American Chem. Soc.* **114**, 3139 (1992).
- [13] X. Ge and R.-B. Wu, Risk-sensitive optimization for robust quantum controls, *Physical Review A* **104**, 012422 (2021).
- [14] L. S. Baker, A. L. P. de Lima, A. Zlotnik, and J.-S. Li, Convergence of Iterative Quadratic Programming for Robust Fixed-Endpoint Transfer of Bilinear Systems, in *63rd IEEE Conference on Decision and Control (CDC)* (IEEE, 2024) pp. 8740–8747.
- [15] I. M. Georgescu, S. Ashhab, and F. Nori, Quantum simulation, *Reviews of Modern Physics* **86**, 153 (2014).
- [16] P. de Fouquieres, S. G. Schirmer, S. J. Glaser, and I. Kuprov, Second order gradient ascent pulse engineering, *Journal of Magnetic Resonance* **212**, 412 (2011).
- [17] M. Vu and S. Zeng, An iterative online approach to safe learning in unknown constrained environments, in *2023 62nd IEEE Conference on Decision and Control (CDC)* (IEEE, 2023) pp. 7330–7335.
- [18] S. Wu, Y.-J. Wang, Q. Diot, and M. Prentiss, Splitting matter waves using an optimized standing-wave light-pulse sequence, *Physical Review A* **71**, 043602 (2005).
- [19] M. Edwards, B. Benton, J. Heward, and C. W. Clark, Momentum-space engineering of gaseous Bose-Einstein condensates, *Physical Review A* **82**, 063613 (2010).
- [20] H. Müller, S.-w. Chiow, and S. Chu, Atom-wave diffraction between the Raman-Nath and the Bragg regime: Effective Rabi frequency, losses, and phase shifts, *Physical Review A* **77**, 023609 (2008).
- [21] M. C. Cassidy, M. G. Boshier, and L. E. Harrell, Improved optical standing-wave beam splitters for dilute Bose-Einstein condensates, *Journal of Applied Physics* **130** (2021).
- [22] A. L. P. de Lima, A. K. Harter, M. J. Martin, and A. Zlotnik, Optimal ensemble control of matter-wave splitting in Bose-Einstein condensates, in *American Control Conference (ACC)* (IEEE, 2024) pp. 4181–4188.